Transforming Growth Factor α Expression Drives Constitutive Epidermal Growth Factor Receptor Pathway Activation and Sensitivity to Gefitinib (Iressa) in Human Pancreatic Cancer Cell Lines

Maria S. Pino,[1,2] Marissa Shrader,[3] Cheryl H. Baker,[3] Francesco Cognetti,[1] Henry Q. Xiong,[2] James L. Abbruzzese,[2] and David J. McConkey[3]

[1]Division of Medical Oncology "A," Regina Elena Cancer Institute, Rome, Italy and Departments of [2]Gastrointestinal Medical Oncology and [3]Cancer Biology, The University of Texas M.D. Anderson Cancer Center, Houston, Texas

Abstract

The epidermal growth factor receptor (EGFR) is considered an important therapeutic target in pancreatic cancer, but it is currently impossible to identify those patients who are most likely to benefit from EGFR-directed therapy. We examined the biological effects of the EGFR tyrosine kinase inhibitor gefitinib (ZD1839, Iressa) in a panel of nine human pancreatic cancer cell lines. The drug strongly inhibited DNA synthesis and induced low levels of apoptosis at clinically relevant concentrations in a subset of three of the lines (L3.6pl, BxPC3, and Cfpac1). Sensitivity to gefitinib correlated directly with ligand [transforming growth factor-α (TGF-α)] expression (r^2 = 0.71, P = 0.004) but not with surface EGFR expression. The gefitinib-sensitive cells displayed constitutive baseline EGFR phosphorylation, whereas the gefitinib-resistant cells did not. Exposure to gefitinib or a small interfering RNA construct specific for TGF-α reversed the constitutive EGFR phosphorylation and downstream target [extracellular signal-regulated kinases (ERK), AKT] phosphorylation in the gefitinib-sensitive cells but had no effects on ERK or AKT phosphorylation in gefitinib-resistant cells. Baseline EGFR phosphorylation was lower in a subclone of L3.6pl selected for low TGF-α expression, and these cells were also resistant to gefitinib-mediated growth inhibition. Gefitinib blocked the growth of tumor xenografts derived from L3.6pl cells but had no effect on the growth of tumors derived from EGFR-independent MiaPaCa-2 cells. Together, our data show that TGF-α expression identifies a subset of human pancreatic cancer cells that is dependent on EGFR signaling *in vitro* and *in vivo*. Quantification of TGF-α expression may therefore represent an effective means of identifying EGFR-responsive primary tumors. (Cancer Res 2006; 66(7): 3802-12)

Introduction

The epidermal growth factor (EGF) receptor (EGFR) is a transmembrane glycoprotein with an extracellular ligand-binding domain, a hydrophobic membrane-spanning domain, and a cytoplasmic domain that harbors tyrosine kinase activity. Binding of specific ligands, such as EGF, transforming growth factor-α (TGF-α), or amphiregulin, to the extracellular domain results in EGFR dimerization, autophosphorylation of the tyrosine kinase domain, and internalization, resulting in activation of downstream signaling pathways that are involved in cell proliferation and survival (1–4). The idea that the EGFR pathway plays a central role in solid tumor progression is suggested by the observation that many human epithelial cancers, including breast, head and neck, non–small cell lung cancer, renal, ovarian, colon and gastric cancer, and gliomas, exhibit amplification/overexpression of the EGFR and increased expression of receptor ligands (2, 5–9). EGFR overexpression occurs in 30% to 50% of human pancreatic adenocarcinomas, correlating with rapidly progressive disease, resistance to chemotherapy, and poor prognosis (10–14).

Gefitinib (also known as ZD1839 or Iressa, AstraZeneca, Macclesfield, United Kingdom) is an orally active, reversible, competitive inhibitor of the EGFR tyrosine kinase ATP-binding site that was developed for cancer therapy (15). Unfortunately, recent clinical trials showed that therapy with gefitinib did not improve patient outcomes when the drug was combined with cytotoxic agents in first-line therapy and did not prolong survival compared with placebo in pretreated patients with advanced non–small cell lung cancer (16–18). These observations and others have undermined enthusiasm for the drug and other EGFR inhibitors in solid tumor therapy. However, other recent work showed that a subset of non–small cell lung cancers, colorectal cancers, and glioblastomas are highly sensitive to single-agent therapy with gefitinib and that many of these tumors contain somatic activating mutations in exons 18 to 21 within EGFR ATP-binding domain (19–22), raising the possibility that subsets of solid tumors with the appropriate biological characteristics might be exquisitely sensitive to the drug. Importantly, disease stability and symptomatic improvement can be achieved in non–small cell lung cancer patients whose tumors do not contain *EGFR* mutations, indicating that mechanisms aside from mutation of the EGFR tyrosine kinase domain must also dictate drug sensitivity.

Here, we examined the effects of gefitinib on cell growth in a panel of nine human pancreatic cancer cell lines. We then examined the biological properties associated with gefitinib sensitivity in an attempt to identify biomarkers associated with sensitivity to the EGFR antagonist. Our data indicate that a subset of cell lines is dependent on TGF-α-mediated activation of the EGFR for cell proliferation and strongly suggest that pancreatic tumors expressing high levels of TGF-α and phosphorylated (activated) EGFR are EGFR-dependent *in vitro* and *in vivo*.

Requests for reprints: David McConkey, Department of Cancer Biology, The University of Texas M.D. Anderson Cancer Center, 1515 Holcombe Boulevard, Unit 173, Houston, TX 77030. Phone: 713-792-8591; Fax: 713-792-8747; E-mail: dmcconke@mdanderson.org.

doi:10.1158/0008-5472.CAN-05-3753

Materials and Methods

Reagents. Gefitinib was purchased from The University of Texas M.D. Anderson pharmacy. Stock solutions were prepared in DMSO and stored at −20°C. Recombinant human EGF and TGF-α ELISA kits were purchased from EMB Biosciences (San Diego, CA). The antibody used for immunohistochemistry and Western blot analyses were from the following sources: mouse anti–proliferating cell nuclear antigen (PCNA) clone PC10 was from DAKO (Copenhagen, Denmark); rabbit anti-total EGFR, rabbit anti-pEGFR (Tyr^{1068}), rabbit anti-total AKT, rabbit anti-pAKT (Ser^{473}), rabbit anti-total mitogen-activated protein kinase (MAPK), and mouse anti-pMAPK (Thr^{202}-Tyr^{204}) were from Cell Signaling Technology (Beverly, MA); mouse anti-TGF-α was purchased from EMB Biosciences; and lamin A/C was from Santa Cruz Biotechnology (Santa Cruz, CA).

Cell lines and culture conditions. The human pancreatic cancer cell lines Aspc1, BxPC3, Capan2, Cfpac1, Hpaf2, HS766T, MiaPaCa-2, and Panc-1 were obtained from the American Type Culture Collection (Manassas, VA). The L3.6pl human pancreatic cancer cell line was established from COLO-357 cells as previously described (23). L3.6pl clones expressing low levels of TGF-α as measured by Northern blot and ELISA analyses were generated by one of us (C.H. Baker) by limiting dilution. The BxPC3 cell line was maintained in RPMI 1640 (Life Technologies, Inc., Gaithersburg, MD). All of the other cell lines were maintained in MEM. The media were supplemented with 10% fetal bovine serum (FBS; Life Technologies), sodium pyruvate (Bio Whittaker, Rockland, ME), L-glutamine (Bio Whittaker), nonessential amino acids (Life Technologies), vitamins (Life Technologies), and antibiotics (penicillin/streptomycin; Bio Whittaker). Adherent monolayer cultures were incubated at 37°C in a mixture of 5% CO_2 and 95% air.

Analysis of EGFR mutations. PCR was used to amplify exons 18, 19, 20, and 21 from the human *EGFR* gene using genomic DNA isolated from each of the cell lines. PCR amplicons were purified using QIAquick PCR purification kit (Qiagen, Valencia, CA). PCR products were sequenced, and the results were blasted and compared with the wild-type *EGFR* sequence from Genbank.

Detection of EGFR cell surface expression by flow cytometry. Cells were harvested, incubated for 1 hour at 4°C with the anti-EGFR monoclonal antibody (mAb) C225 (ImClone Systems Incorporated, Somerville, NJ), and washed twice with ice-cold PBS containing 0.5% bovine serum albumin (BSA). After 1-hour incubation at 4°C in the dark with AlexaFluor-488-conjugated goat anti-human IgG antibody (Invitrogen Corp., Carlsbad, CA), cells were washed, resuspended in ice-cold PBS/BSA, and analyzed by flow cytometry (Beckman-Coulter, Miami, FL). The Coulter software was used to determine mean fluorescence intensities.

[^{3}H]thymidine proliferation assay. Cells were plated in 96-well plates at a density of 1×10^4 per well. Cells were exposed 24 hours later to various concentrations of gefitinib (0.1-10 μmol/L) in serum-free MEM. After 24 hours, the medium was removed and replaced with fresh MEM containing 10% FBS and 10 μCi/mL [^{3}H]thymidine (Amersham Biosciences, Piscataway, NJ). The cells were pulsed with [^{3}H]thymidine for 1 hour, lysed by the addition of 0.1 N KOH, and harvested onto fiberglass filters. The incorporated tritium was quantified in a scintillation counter.

Cell cycle analysis. Cells were growth in six-well plates in the presence of 10% MEM. After reaching 70% confluence, the cells were exposed to various concentrations of gefitinib for 24 hours. Cells were harvested by trypsinization and pelletted by centrifugation. The pellets were then resuspended in PBS containing 50 μg/mL propidium iodide, 0.1% Triton X-100, and 0.1% sodium citrate. Samples were stored at 4°C for 1 hour before analysis. Propidium iodide fluorescence was measured by fluorescence-activated cell sorting (FACS) analysis (FACScan FL-3 channel; Becton Dickinson, Mountain View, CA) as described previously (24). Cells displaying a hypodiploid content of DNA indicative of DNA fragmentation were scored as apoptotic.

Small interfering RNA–mediated knockdown of TGF-α. L3.6pl cells were grown in six-well plates until they reached 40% confluence and then transfected with small interfering RNA (siRNA) targeting endogenous TGF-α and unrelated targets using OligofectAMINE (Invitrogen). All the siRNA constructs were obtained from Dharmacon Research, Inc. (Lafayette, CO). The TGF-α siGENOME SMARTpool reagent was used to knockdown TGF-α expression. Functional nontargeting siRNAs (siCONTROL Non-Targeting Pool) was used to show that transfection did not induce nonspecific effects on gene expression. We used siRNA directed against lamin A/C as an off-target control.

Immunoblot analyses. Cells were scraped from tissue culture plates with a rubber policeman into Triton lysis buffer [1% Triton X-100, 150 mmol/L NaCl, 25 mmol/L Tris (pH 7.5), 1 mmol/L glycerol phosphate, 1 mmol/L sodium orthovanadate, 1 mmol/L sodium fluoride, and one Complete Mini Protease Inhibitor Cocktail tablet (Roche, Indianapolis, IN)] and were incubated for 1 hour on ice. The lysates were then clarified by centrifugation before resolution by 10% SDS-PAGE. Polypeptides were transferred to nitrocellulose membranes. Membranes were blocked in 5% nonfat milk in a TBS containing 0.1% Tween 20 (TBS-T) for 2 hours at 4°C, incubated overnight with relevant antibodies, washed, and probed with species-specific secondary antibodies coupled to horseradish peroxidase (Amersham Biosciences), and detected by enhanced chemiluminescence (Renaissance, New England Nuclear, Boston, MA).

Immune complex cdk-2 kinase assay. Cells were cultured in 10 cm dishes and exposed to 1 μmol/L gefitinib for various periods of time. Cells were then harvested with trypsin and lysed for 1 hour at 4°C in the Triton X-100 lysis buffer described above. After centrifugation, the clarified supernatants were incubated with an anti cdk-2 antibody for 2 hours followed by overnight incubation at 4°C with protein G-Sepharose beads (Santa Cruz Biotechnology). The immune complexes were washed twice with lysis buffer and once with kinase buffer [25 mmol/L Tris (pH 7.2) and 10 mmol/L $MgCl_2$]. Immunoprecipitates were incubated with 1 μg histone H1, 150 μmol/L ATP, and 10 μCi [γ-^{32}P]ATP in 50 μL kinase buffer for 15 minutes at room temperature. SDS sample buffer was used to terminate the reactions, samples were boiled for 5 minutes, and the mixtures were loaded onto 12% SDS-PAGE gels. The gels were stained with Coomassie blue, destained, and dried, and radiolabeled histone H1 was detected by autoradiography.

Effects of gefitinib on tumor growth. Six-week-old male athymic nude mice (NCr-*nu*) were purchased from the Animal Production Area of the National Cancer Institute-Frederick Cancer Research and Development Center (Frederick, MD). L3.6pl cells and MiaPaCa-2 (1×10^6/100 μL HBSS) were injected s.c. into the dorsal flank areas of the mice. When the tumors reached 0.3 cm^3, mice were randomized into two treatment groups of 10 mice each: The first control group received vehicle solution, whereas the second group received 100 mg/kg gefitinib, both for 5 d/wk by i.p. injection. Tumor volumes were determined weekly using a caliper and the following formula: $V = \pi$ (smaller diameter)^2 (larger diameter) / 6. Mice were euthanized and primary tumors were excised and weighed. For immunohistochemistry, one part of the tumor tissue was formalin-fixed and paraffin-embedded, another part was embedded in optimum cutting temperature compound (Miles, Inc., Elkhart, IN), frozen rapidly in liquid nitrogen, and stored at −80°C.

Immunohistochemical analysis. Paraffin-embedded tissues were used for identification of PCNA, total and phosphorylated EGFR, TGF-α, and total and phosphorylated Akt. Sections (4-6 μm thick) were mounted on positively charged Superfrost slides (Fisher Scientific, Houston, TX) and dried overnight. Sections were deparaffinized in xylene, treated with a graded series of alcohol [100%, 95% and 80% ethanol/double-distilled H_20 (v/v)], and rehydrated in PBS (pH 7.5). Sections analyzed for PCNA were microwaved for 5 minutes for antigen retrieval (25). All samples were incubated with 3% hydrogen peroxide in methanol (v/v) for 12 minutes to block endogenous peroxidase, washed with PBS (pH 7.5), and incubated in protein blocking solution (5% normal human serum, 1% normal goat serum in PBS, v/v) for 20 minutes. The sections were incubated with the appropriate primary antibody in a humidified chamber overnight at 4°C, rinsed with PBS, and incubated in protein blocking solution for 10 minutes. Sections were then incubated for 60 minutes with the corresponding peroxidase-conjugated secondary antibody at room temperature. Positive reactions were visualized by incubating the slides with stable 3,3′-diaminobenzidine (Research Genetics, Huntsville, AL) for 7 to 10 minutes. The reactions were terminated by rinsing the slides with distilled water.

The slides were counterstained with Gill's hematoxylin (Sigma Chemical) for 10 seconds, mounted with Universal Mount (Research Genetics), and dried on a 56°C hot plate. Sections stained for TGF-α were preincubated with goat anti-mouse IgG F(ab)$_2$ fragment (1:10 dilution in PBS) overnight at 4°C before the incubation with the primary antibody. Frozen tissues used for identification of total and phosphorylated MAPK were sectioned (8-10 μm), mounted on positively charged Plus slides (Fisher Scientific), and air-dried for 30 minutes. Frozen sections were fixed in cold acetone (5 min), acetone/chloroform (v/v; 5 min), and acetone (5 min), and washed with PBS. Slides were blocked with PBS supplemented with 5% normal human serum and 1% normal goat serum for 20 minutes and incubated with the primary antibody in a humidified chamber overnight at 4°C. The slides were then rinsed with PBS and incubated with goat anti-rabbit Alexa 488 for 1 hour at room temperature. After PBS washes, Hoechst nuclear counterstain was applied. To quantify PCNA expression, the number of positive cells was counted in 10 random 0.159 mm^2 fields at ×100 magnification. To quantify the intensity of immunohistochemical reactions, the absorbances of six positive cells per field in 10 random 0.159 mm^2 fields at ×100 magnification of different treated tumor tissues were measured. Microscopy was done using a Nikon Microphot-FXA microscope (Nikon, Inc., Garden City, NY), and images were captured using a cooled charge-coupled device Hamamatsu 5810 camera (Hamamatsu Corp., Bridgewater, NJ) and Optimas Image Analysis software (Media Cybernetics, Silver Spring, MD). Immunofluorescence microscopy was done using a ×20 objective on an epifluorescence microscope equipped with a narrow band-pass excitation filter mounted in a filter wheel (Ludl Electronic Products, Hawthorne, NY). Photomontages were prepared using Adobe Photoshop software (Adobe Systems, Inc., San Jose, CA).

Statistical analysis. All assays done in this study were conducted at least thrice. Numerical data are presented as mean ± SE. Comparisons between test and control groups were evaluated using Student's t test. Statistical significance was set at $P < 0.05$.

Results

Effects of gefitinib on the growth of pancreatic cancer cell lines *in vitro*. Previous studies showed that EGFR inhibitors arrest responsive cell lines within the G_1 phase of the cell cycle *in vitro* (26, 27). We therefore used [^{3}H]thymidine incorporation assays to measure rates of DNA synthesis in cells exposed to increasing concentrations of gefitinib (0.1-10 μmol/L) as a means of identifying the responsive cell lines within our panel. We observed significant heterogeneity in drug responsiveness, with only three of nine cell lines (L3.6pl, BxPC3, and Cfpac1) displaying at least a 50% inhibition of DNA synthesis (IC_{50}) at concentrations of ZD1839 ≤1 μmol/L (Table 1). We obtained independent confirmation of these results by measuring the accumulation of cells in G_1 by propidium iodide staining and FACS analysis. As shown in Table 2, gefitinib induced increases in G_1 with corresponding decreases in S phase in the three cell lines that displayed significant decreases in DNA synthesis in the [^{3}H]thymidine incorporation assays (L3.6pl, BxPC3, and Cfpac1), whereas it had no effect on cell cycle progression in the MiaPaca-2 or Panc-1 cells. Other work has shown that EGFR inhibitors can induce apoptosis in drug-sensitive tumor cells (28–30). However, the percentage of cells in the sub-G_0-G_1 population was relatively modest, suggesting that gefitinib exerts largely cytostatic effects on these cells (Fig. 1*A*).

In an attempt to identify the molecular events responsible for the G_1 block observed in the gefitinib-sensitive cells, we measured the effects of the drug on expression of the cyclin-dependent kinase inhibitor p27^{Kip1} and on cdk-2 kinase activity. Gefitinib induced a time-dependent accumulation of p27^{Kip1} in the drug-sensitive cell lines L3.6pl, BxPC3, and CfPac1, but not in the drug-resistant MiaPaCa-2 or Panc-1 cells (Fig. 1*B*). Accumulation of p27^{Kip1} was associated with an inhibition of cdk-2 kinase activity (Fig. 1*B*).

Expression of EGFR and TGF-α. We used the antihuman EGFR antibody C225 and flow cytometry to determine the levels of

Table 1. Effect of ZD1839 on DNA synthesis

Cell lines	ZD1839 (μmol/L)		
	0.1	1	10
L3.6p1	54	23	10
BxPC3	49	29	9
CfPac1	87	49	13
HS766T	88	68	38
Hpaf2	98	81	46
Aspc1	76	64	52
MiaPaCa-2	86	82	54
Panc-1	83	81	60
Capan2	87	83	61

NOTE: Results are expressed as percentage of cell number compared with the same cell line growth in the absence of the drug. In the raw data, the SE did not exceed 10%.

Table 2. Effect of ZD1839 on cell cycle distribution

Cell lines	%G_1	%S	%G_2
L3.6p1			
Control	67	29	4
ZD1839, 1 μmol/L	78	17	5
ZD1839, 10 μmol/L	84*	10†	6
BxPC3			
Control	51	35	14
ZD1839, 1 μmol/L	64†	23†	13
ZD1839, 10 μmol/L	71†	20†	9
CfPac1			
Control	76	14	10
ZD1839, 1 μmol/L	80	10	10
ZD1839, 10 μmol/L	84*	7*	9*
MiaPaCa-2			
Control	73	12	15
ZD1839, 1 μmol/L	74	12	14
ZD1839, 10 μmol/L	76	9	15
Panc-1			
Control	63	13	24
ZD1839, 1 μmol/L	62	14	24
ZD1839, 10 μmol/L	63	13	24

NOTE: Cell cycle analysis of cells treated with 1 and 10 μmol/L ZD1839. Cells were stained with propidium iodide after a 24-hour exposure to ZD1839 and analyzed by flow cytometry. Percentages of the total cell population in the different phases of the cell cycle were determined and included. Mean value of at least three experiments are shown.

*$P < 0.05$.

†$P < 0.001$.

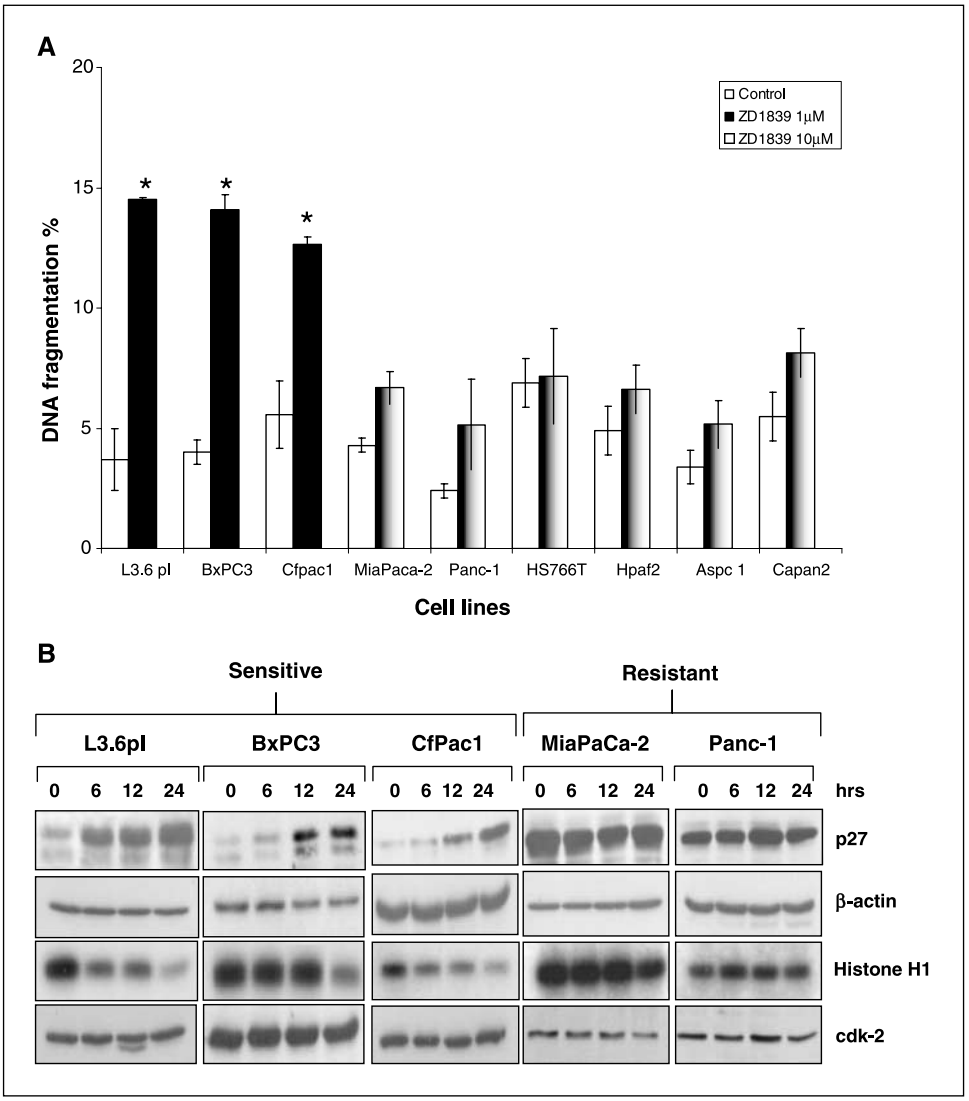

Figure 1. Effects of gefitinib on cell cycle progression and apoptosis. *A,* effects of gefitinib on DNA fragmentation. Cells were incubated in the absence or presence of 1 and 10 μmol/L gefitinib for 24 hours and DNA fragmentation was quantified by propidium iodide/FACS. *Columns,* average of at least three experiments; *bars,* SE. *, $P < 0.001$. *B,* effects of gefitinib on $p27^{Kip1}$ protein expression and cdk-2 activity. Cells were incubated in the absence or presence of 1 μmol/L gefitinib for the indicate times and $p27^{Kip1}$ expression and cdk-2 activity were measured as described in Materials and Methods. Expression of actin and cdk-2 protein were measured by immunoblotting in the same cell lysates and served as loading controls. Gefitinib induced a time-dependent accumulation of $p27^{Kip1}$ in the drug-sensitive cell lines L3.6pl, BxPC3, and CfPac1, but not in the drug-resistant MiaPaCa-2 or Panc-1 cells. Accumulation of $p27^{Kip1}$ was associated with an inhibition of cdk-2 kinase activity.

surface EGFR expressed by our cells. EGFR expression was highly variable, with Aspc1 and Panc-1 displaying the highest levels (mean fluorescence intensities of 100 and 59.5, respectively) and HS766T and MiaPaca-2 the lowest (mean fluorescence intensities of 11.7 and 4.3, respectively; Fig. 2*A*). Thus, there was no relationship between surface EGFR expression and gefitinib sensitivity, consistent with previous conclusions (31–34). To determine whether L3.6pl, BxPC3, or Cfpac1 harbored activating EGFR mutations that might render them more sensitive to gefitinib, we isolated genomic DNA and sequenced exons 18 to 21 of the EGFR expressed by these cells and all of the other lines in the panel. These exons encode the tyrosine kinase domain and contain all of the activating mutations identified in the previous studies (19–21). However, we found no mutations in any of the cell lines (data not shown).

Because we did all of our [^{3}H]thymidine assays with cells cultured in serum-free medium (i.e., no exogenous ligand), the simplest explanation for our results was that the three gefitinib-sensitive cell lines were dependent on autocrine ligand–EGFR interactions for cell cycle progression and the other six were not. The major autocrine ligand for the EGFR that is expressed by epithelial tumors is TGF-α (8, 9). Therefore, to test our hypothesis, we measured autocrine TGF-α, EGF, and HB-EGF production in our panel of cell lines by ELISA (Fig. 2*B*). Consistent with the [^{3}H]thymidine and cell cycle analyses, L3.6pl and BxPC3 produced the highest constitutive levels of TGF-α (mean = 1,034.21 ± 200 and 561 ± 82 pg/μg protein, respectively). Cfpac-1 produced intermediate levels of TGF-α that were similar to those observed in four of the gefitinib-resistant cells, and the remaining gefitinib-resistant lines (MiaPaCa-2 and Panc-1) produced very little to no detectable TGF-α (Fig. 2*B*). Overall, we observed a direct linear correlation between gefitinib sensitivity and TGF-α production ($r^2 = 0.71$, $P = 0.004$). In contrast, we observed no correlation between cellular EGF or HB-EGF production and gefitinib sensitivity in the panel (data not shown).

Effects of gefitinib on EGFR-related signaling pathways. The observation that constitutive TGF-α expression correlated with gefitinib sensitivity strongly suggested that the EGFR signal transduction pathway was constitutively "on" in the gefitinib-sensitive subset of pancreatic cancer cell lines and not in the others. To directly address this possibility, we compared the levels of baseline EGFR phosphorylation in the cells (Fig. 3*A*). We also

stimulated the cells with exogenous EGF and measured the concentration-dependent effects of gefitinib on EGFR phosphorylation to determine whether differences in gefitinib responsiveness could be shown (Fig. 3*B*). Consistent with our hypothesis, the gefitinib-sensitive L3.6pl, BxPC3, and Cfpac1 cells all displayed significant baseline EGFR phosphorylation when they were grown in serum-free medium, whereas the gefitinib-resistant MiaPaCa-2 and Panc-1 cells did not (Fig. 3*A*). Gefitinib reversed the basal EGFR phosphorylation observed in all three drug-sensitive cell lines (Fig. 3*A*). The effects of gefitinib on EGF-mediated EGFR phosphorylation were very similar across the panel (Fig. 3*B*), indicating that major differences in the receptor responsiveness to gefitinib-mediated inhibition did not underlie the differential drug sensitivity observed.

EGF-induced progression through the G_1-S cell cycle checkpoint is mediated by activation of the extracellular signal-regulated kinase (ERK) and AKT signal transduction pathways (35–37). Therefore, we compared the concentration-dependent effects of gefitinib on ERK and AKT phosphorylation in the gefitinib-sensitive and gefitinib-resistant cell lines. Significant constitutive ERK and AKT phosphorylation were observed in all of the cell lines, consistent with the general importance of these pathways in driving tumor cell proliferation (Fig. 3*A*). Interestingly, exogenous EGF failed to increase phosphorylated ERK or phosphorylated AKT levels in the L3.6pl and BxPC3 cells (Fig. 3*C*), strongly suggesting that the EGF-EGFR pathway was already optimally activated in these cell lines. However, exogenous EGF triggered further increases in ERK and AKT phosphorylation in the Cfpac1, MiaPaCa-2, and Panc-1 cells that were reversed by gefitinib in a concentration-dependent fashion (Fig. 3*C*). Conversely, ZD1839 strongly inhibited constitutive ERK and AKT phosphorylation in L3.6pl, BxPC3, and Cfpac1 cells grown in serum-free medium, whereas it had no effect on baseline ERK and AKT phosphorylation in the MiaPaCa-2 and Panc-1 cells (Fig. 3*A*). Together, these data

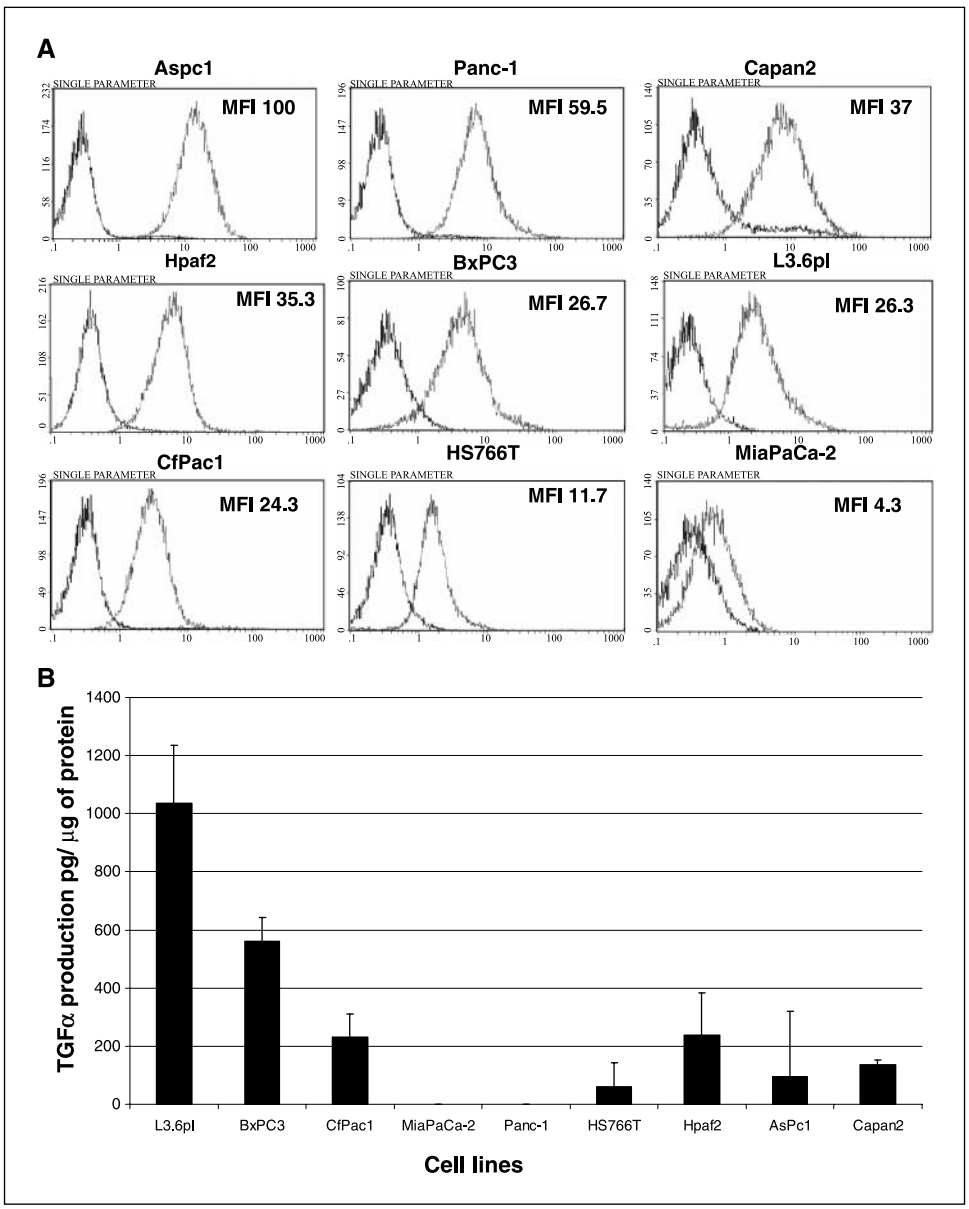

Figure 2. Relationship between EGFR and TGF-α expression and ZD1839 sensitivity. *A,* surface EGFR expression. To quantify receptor expression, intact cells were stained with an EGFR mAb (C225) and fluorescence was measured by FACS. Representative FACS histograms are shown. *Blue traces,* antibody controls (*background staining*); *red peaks,* EGFR-specific fluorescence. Mean fluorescence intensities (*MFI*) were calculated for each cell line (*top right corner*) and are averages of at least three experiments. *B,* cellular TGF-α production. Ligand levels were measured by ELISA in cells maintained in serum-free medium for 24 hours. *Columns,* mean from at least three experiments; *bars,* SE.

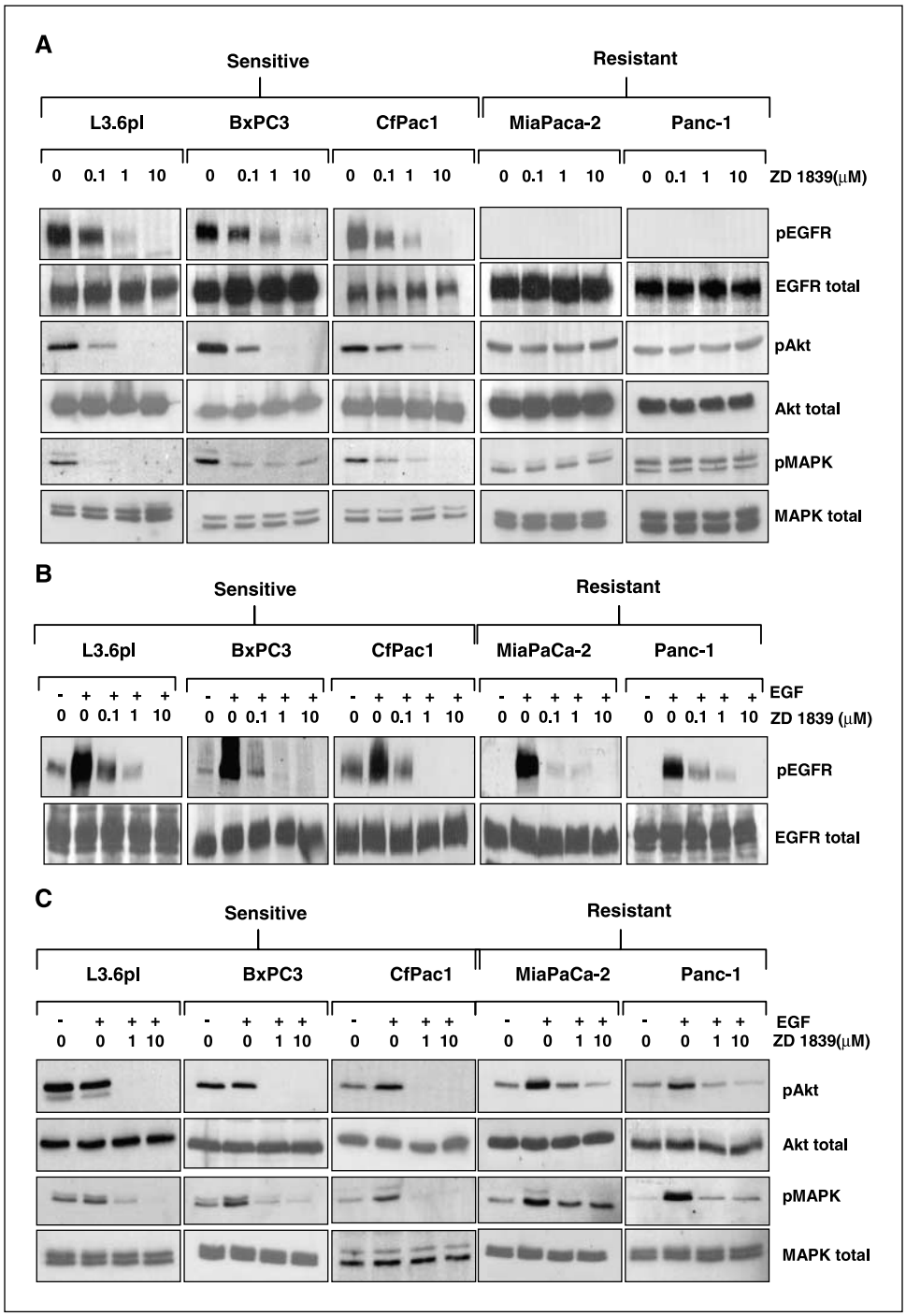

Figure 3. Status of EGFR pathway activation in ZD1839-sensitive and ZD1839-resistant cells. *A,* effects of gefitinib on baseline ERK and AKT phosphorylation. Serum-starved cells were incubated with the indicated concentrations of gefitinib and antigen expression was measured by immunoblotting. Note that gefitinib completely inhibited baseline ERK and AKT phosphorylation in the gefitinib-sensitive cells but had no effect on the gefitinib-resistant cells. *B,* concentration-dependent effects of gefitinib on EGF-induced phosphorylation of EGFR. Cells were serum-starved overnight and preincubated with the indicated concentrations of gefitinib for 2 hours. Cells were then incubated with 20 ng/mL EGF for 15 minutes, and EGFR phosphorylation was measured by immunoblotting using a phosphorylation-specific antibody. Immunoblotting for total EGFR was done to control for protein loading. *C,* concentration-dependent effects of gefitinib on ERK and AKT phosphorylation in gefitinib-sensitive and gefitinib-resistant cell lines. Serum-starved cells were incubated with the indicated concentrations of gefitinib and then incubated with EGF (20 ng/mL) for 15 minutes. Protein extracts were resolved by 10% SDS-PAGE and target phosphorylation was measured by immunoblotting using phosphorylation-specific antibodies. The results revealed concentration-dependent inhibition of EGF-induced ERK and AKT phosphorylation in all of the cell lines. Note that total ERK and AKT levels were not altered by gefitinib.

strongly suggest that constitutive EGFR activation drives ERK and AKT phosphorylation in the gefitinib-sensitive pancreatic cancer lines. Other mechanisms must account for the constitutive ERK and AKT phosphorylation observed in the gefitinib-resistant cells.

Effects of TGF-α modulation on EGFR pathway activity and sensitivity to gefitinib. To more directly determine the relationship between TGF-α expression and sensitivity to gefitinib, we knocked down TGF-α expression in L3.6pl cells via RNA interference and compared cellular responsiveness to gefitinib in silenced cells and controls. Quantification of cellular TGF-α levels by ELISA confirmed that silencing was very efficient (80% inhibition; Fig. 4*A*). Constitutive EGFR, ERK, and AKT phosphorylation were strongly reduced in L3.6pl cells transfected with the TGF-α-specific siRNA construct relative to the levels observed in the untreated cells, cells transfected with a nontargeting control, or cells transfected with an off-target control (lamin A/C), confirming that TGF-α was directly responsible for receptor and downstream pathway activation (Fig. 4*A*). Furthermore, baseline [^{3}H]thymidine uptake was lower in the TGF-α-silenced cells versus control siRNA-treated cells (2,612 ± 322 cpm/10^5 cells versus 3,509 ± 669, $P < 0.05$), and gefitinib had no further effect on [^{3}H]thymidine incorporation in the TGF-α-silenced cells (Fig. 4*B*).

In a second series of experiments, we compared the gefitinib responsiveness of the parental L3.6pl cells to a subclone of L3.6pl that spontaneously expresses reduced levels of TGF-α (130.75 ± 32 pg/μg protein in the subclone versus 639.95 ± 6.6 pg/μg protein in the parental L3.6pl cells, or an 80% reduction). The subclone expressed lower levels of phosphorylated EGFR, ERK, and AKT at baseline than the parental cells (data not shown) and was also significantly less sensitive to gefitinib-mediated growth inhibition (Fig. 4*C*).

Effects of gefitinib on the growth of L3.6pl and MiaPaCa-2 xenografts. Previous studies have shown that EGFR antagonists inhibit angiogenesis in preclinical models of human pancreatic cancer (38, 39). Thus, it is conceivable that EGFR-directed therapy can be effective whether the tumor cells themselves are dependent on EGFR signaling for proliferation. To address this possibility, we compared the effects of gefitinib therapy on the growth of drug-sensitive L3.6pl and drug-resistant MiaPaca-2 tumors growing *in vivo*. We initiated therapy when the tumors had reached 0.3 cm^3 and treated the mice daily via i.p. injection with a fairly high dose of the drug (100 mg/kg). As shown in Table 3 and Fig. 5*A*, gefitinib did not produce cumulative toxicity or changes in body weight at this dose but did significantly inhibit the growth of L3.6pl tumors compared with those isolated from mice treated with vehicle alone ($P < 0.05$). All mice in the control group showed progressive disease and were sacrificed early because of tumor burden. Gefitinib seemed to exert largely cytostatic effects on the L3.6pl tumors, as has been reported previously (26, 27). The mean number of PCNA-positive cells per high power field in the L3.6pl tumors was reduced from 190.8 ± 35 in the control group to 57.1 ± 13 in tumors exposed to 100 mg/kg gefitinib ($P < 0.001$). On the other hand, gefitinib had no effect on the growth of the MiaPaCa-2 tumors, and all mice were sacrificed after 2 weeks because of tumor burden. Gefitinib also had no detectable effect on proliferation in the MiaPaCa-2 tumors, as the mean number of PCNA-positive cells per high power field was 85.4 ± 12 and 84.2 ± 9 in tumors harvested from control and gefitinib-treated tumors, respectively.

Finally, we assessed the effects of gefitinib therapy on EGFR, ERK, and AKT phosphorylation in L3.6pl and MiaPaCa-2 tumors by immunohistochemistry. Initial studies confirmed that TGF-α levels were high in the L3.6pl tumors but were nearly undetectable in the MiaPaCa-2 tumors (Fig. 5*B*), analogous to the patterns of TGF-α expression observed in the two cell lines *in vitro* (Fig. 2*B*). Furthermore, the effects of gefitinib on protein kinase activation *in vivo* were nearly indistinguishable from the effects observed in the two cell lines *in vitro*. Specifically, in L3.6pl tumors, we observed marked reductions in EGFR, ERK, and AKT phosphorylation in

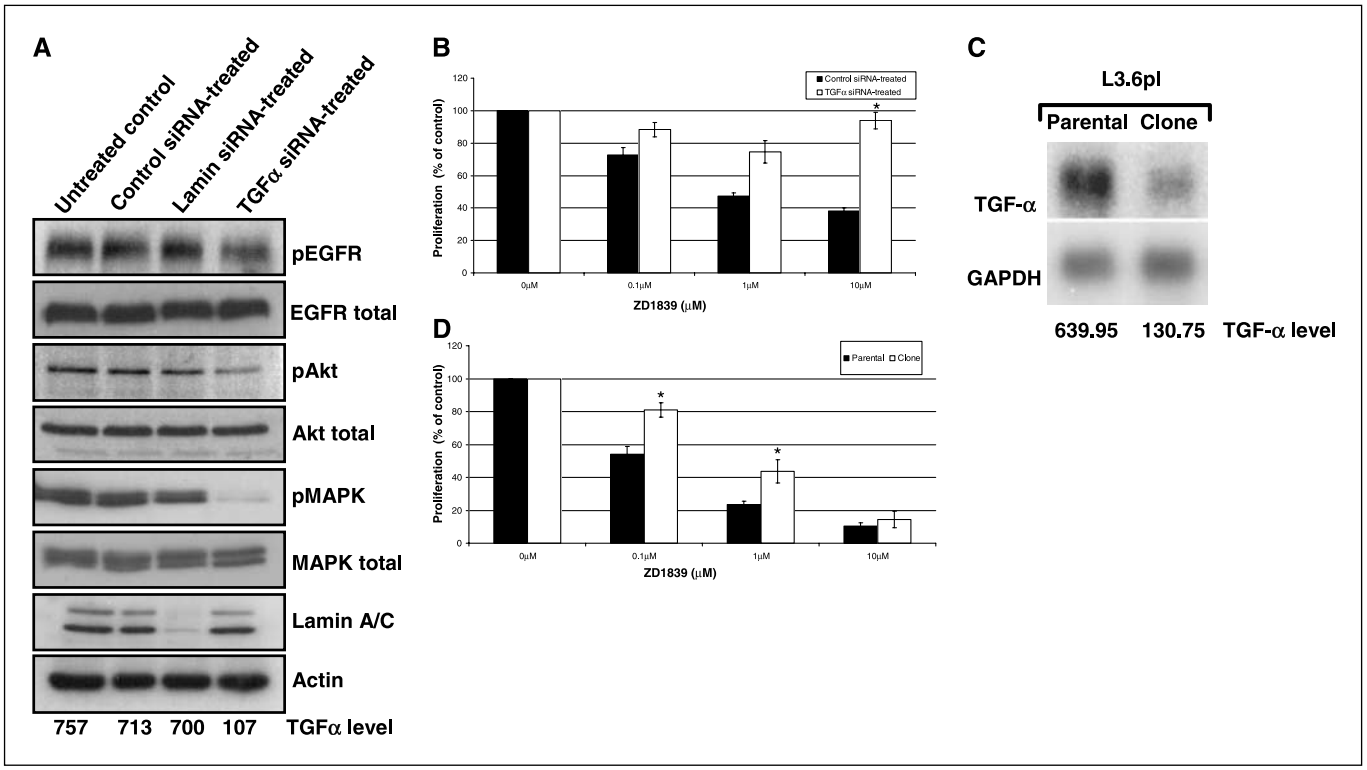

Figure 4. Effects of reducing TGF-α levels on gefitinib sensitivity. *A,* effects of TGF-α silencing on EGFR pathway activation in L3.6pl cells. Protein extracts from untransfected cells and cells transiently transfected with functional nontargeting siRNAs, lamin A/C siRNA or TGF-α siRNA, were prepared 48 hours after transfection. Levels of phosphorylated EGFR, ERKs, and AKT were compared in the cells by immunoblotting. The effects of TGF-α knockdown on TGF-α levels were measured by ELISA (*numbers below the immunoblots*). Note that TGF-α knockdown reduced levels of all three activation markers, indicating that constitutive TGF-α caused baseline EGFR activation in the cells. *B,* effects of TGF-α silencing on gefitinib sensitivity. L3.6pl cells were transfected with functional nontargeting siRNAs or a TGF-α-selective siRNA construct. Forty-eight hours later, the concentration-dependent effects of gefitinib on DNA synthesis were evaluated by [^{3}H]thymidine incorporation as outlined in Materials and Methods. Note that TGF-α knockdown reduced baseline [^{3}H]thymidine incorporation from 3,509 ± 669 to 2,612 ± 322 cpm/10^5 cells in the control versus TGF-α-silenced cells, respectively. Values displayed are normalized to these control values. *C,* L3.6pl cells that naturally express low TGF-α levels were isolated by limiting dilution. Parental L3.6pl cells and L3.6pl subclones were analyzed for TGF-α expression by Northern blot and ELISA. *D,* concentration-dependent effects of gefitinib on DNA synthesis in L3.6pl parental cells and subclones. Cells were exposed to increasing concentrations of gefitinib for 24 hours in serum-free medium, and DNA synthesis was measured by [^{3}H]thymidine incorporation as described in Materials and Methods. Results are standardized relative to controls. *Columns,* mean from at least three independent experiments; *bars,* SE.

Table 3. Antitumor activity of ZD1839 against human xenografts in nude mice

	Tumor volume (mm^3)		Tumor weight (g)		Body weight (g)	
	Mean	Range	Mean	Range	Mean	Range
L3.6p1						
Control*	1,364	1,204-1,524	1.1	1-1.1	24.1	22.3-25.8
ZD1839†	615.67	451-780‡	0.2	0.2-0.2‡	24.5	23.2-25.8
MiaPaCa-2*						
Control	1,025	868-1,182	0.6	0.5-0.8	29.8	27.7-32.2
ZD1839	1,035	1,033-1,138	0.5	0.4-0.6	28.1	27.8-28.3

NOTE: L3.6p1 and MiaPaCa-2 human pancreatic cancer cells (1×10^6) were injected s.c. into the dorsal flank area of nude mice. When the tumors reached 0.3 cm^3, mice were randomized into two treatment groups of 10 mice each: the first control group received vehicle solution, whereas the second group received 100 mg/kg ZD1839 for 5 d/wk by i.p. injection.

*Mice were sacrificed after 2 weeks of treatment.

†Mice were sacrificed after 4 weeks of treatment.

‡$P < 0.05$ compared with control.

response to gefitinib therapy, whereas the drug had no significant effects on any of the markers in the MiaPaCa-2 tumors. Quantitative analyses of immunohistochemical staining intensities are summarized in Table 4.

Discussion

Cancer of the exocrine pancreas is the fourth leading cause of cancer-related death in the United States (40). Our inability to detect pancreatic cancer at an early stage, the inherent aggressiveness of the disease, and the lack of effective systemic therapies are responsible for the nearly identical incidence and mortality rates observed. Adjuvant therapy has little effect on mortality, and the current frontline agent (the deoxycytidine analogue gemcitabine) provides symptomatic improvement but does not extend median survival beyond 6 months (41). Thus, the development of more effective, biology-based therapies is desperately needed.

The EGFR is overexpressed by a large percentage of primary pancreatic tumors in a manner that correlates with disease progression and resistance to conventional therapy (10–14). Furthermore, previous studies with EGFR antagonists in orthotopic L3.6pl xenografts showed that they strongly inhibit tumor growth via mechanisms that involve direct effects on tumor cells and indirect effects exerted through inhibition of angiogenesis (38, 39). Unfortunately, recent clinical experience with gefitinib and other EGFR antagonists in pancreatic cancer patients has been largely disappointing (42). Therefore, we wondered whether tumor heterogeneity might limit the number of primary tumors that could potentially respond to EGFR-directed therapy. Identification of the factor(s) that engender EGFR dependency could enable us to prospectively identify those tumors that are most likely to respond to gefitinib and other EGFR antagonists.

In an effort to address this hypothesis, we investigated the growth inhibitory effects of gefitinib in a panel of nine human pancreatic cancer cell lines. Our results confirmed that a minority (three of nine) of the cell lines displays significant sensitivity to pharmacologically and clinically relevant concentrations of gefitinib (≤1 μmol/L) as measured by two independent assays for G_1-S cell cycle arrest. Importantly, we observed a linear correlation between gefitinib sensitivity and TGF-α expression in our cell lines, strongly suggesting that autocrine TGF-α production drove EGFR pathway dependency. We obtained additional evidence for the existence of this relationship by comparing the gefitinib sensitivities of parental L3.6pl cells and a subclone that constitutively produced lower levels of TGF-α, in that the former was much more sensitive to gefitinib-mediated growth arrest than the latter. Finally, using a siRNA construct directed against TGF-α, we confirmed that a causal relationship exists between cellular TGF-α production and EGFR pathway activation and proliferation in the L3.6pl cells. Thus, our results show that TGF-α expression identifies those human pancreatic cancer cell lines that exhibit constitutive EGFR pathway activation and are sensitive to EGFR antagonists *in vitro*. Our data would predict that TGF-α expression would also directly correlate with constitutive EGFR, ERK, and AKT phosphorylation and sensitivity to gefitinib-mediated growth arrest in primary patient tumors, and we plan to test this hypothesis in future studies.

In agreement with previous reports, our data show that the level of total EGFR expression does not correlate with gefitinib sensitivity. For example, we found that the Panc-1 and Aspc1 express relatively high surface EGFR levels, but both displayed EGFR resistance (gefitinib IC_{50} >10 μmol/L) in all of our functional assays (31–34). The lack of a relationship between surface EGFR levels and sensitivity to EGFR inhibition stands in contrast to our findings in human bladder cancer cell lines, where we found that gefitinib-sensitive cells expressed significantly higher levels of surface EGFR than did gefitinib-resistant cells.[4] The situation is also different from that observed with another erbB family member in human breast cancer, where expression of erbB2/HER-2 correlates with responsiveness to the anti-HER2/neu receptor mAb trastuzumab (43, 44). Therefore, it seems that some human pancreatic cancer cell lines express high EGFR levels but the receptor is not activated at baseline. Whether ligand provided by the *in vivo* microenvironment would render them EGFR-dependent and gefitinib-sensitive is an issue that requires additional investigation.

Although gefitinib did induce increases in apoptosis in the three cell lines that were most strongly growth arrested by the drug, the levels of cell death were much lower than the degree of growth arrest observed. Furthermore, gefitinib produced largely cytostatic effects

[4] M. Shrader, in preparation.

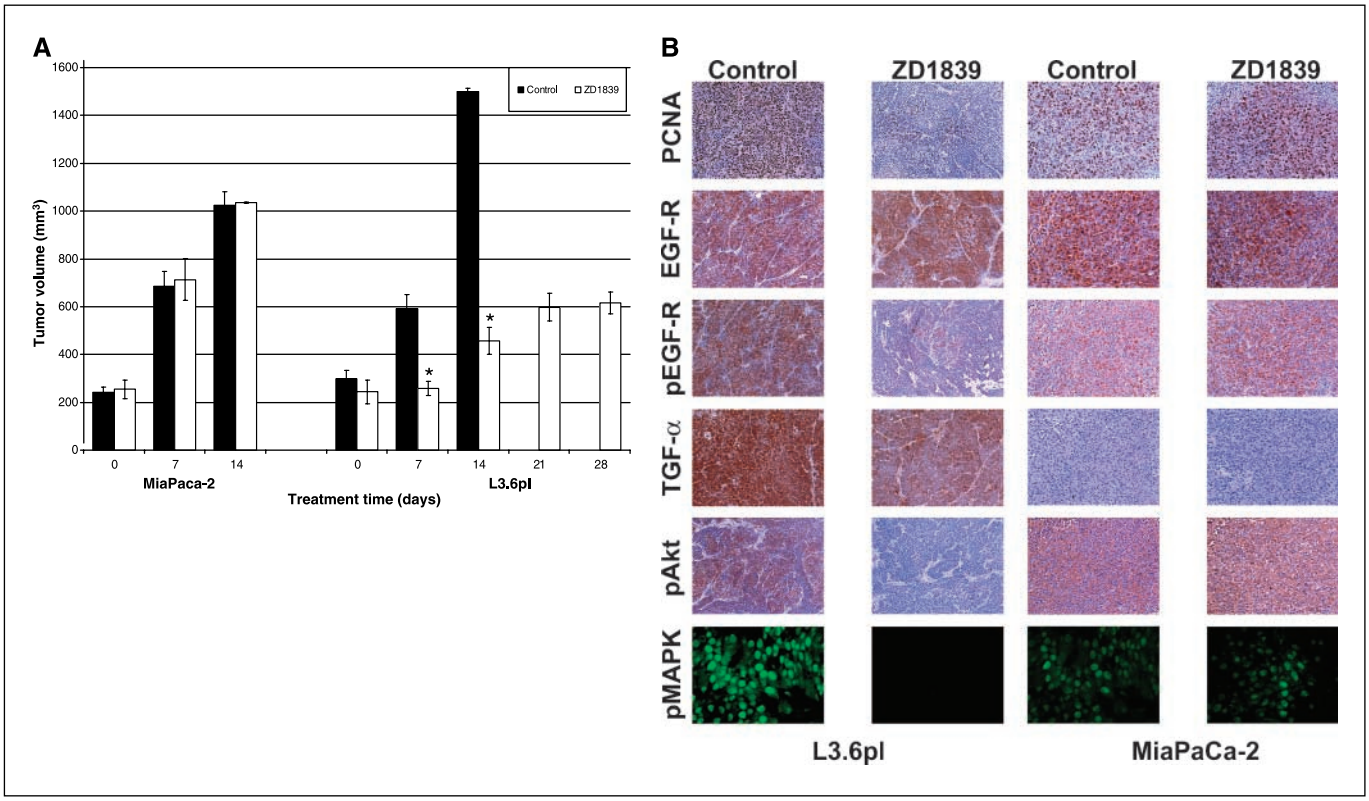

Figure 5. Effects of gefitinib therapy on the growth of L3.6pl and MiaPaCa-2 tumors *in vivo. A,* tumor growth curves. S.c. L3.6pl and MiaPaca-2 tumor xenografts were treated with 100 mg/kg gefitinib as described in Materials and Methods. Gefitinib significantly reduced tumor growth in L3.6pl tumors compared with mice treated with vehicle alone ($P < 0.05$), whereas it had no effect on the growth of the MiaPaca-2 tumors. *B,* effects of gefitinib on proliferation and EGFR pathway activity *in vivo*. The effects of therapy on proliferation were measured by staining tumors with an antibody specific for PCNA. Tumors were also analyzed for expression of TGF-α, total and activated EGFR, phosphorylated AKT, and phosphorylated MAPK as described in Materials and Methods. Representative results are shown.

on the growth of L3.6pl tumors *in vivo*, a finding that is consistent with the conclusions of others (26, 27). Therefore, the most obvious effects of gefitinib seem to involve cell cycle arrest in G_1 or at the G_1-S checkpoint associated with accumulation of p27 and inhibition of cdk-2 activity. This cell cycle arrest could have important implications for the outcome of single-agent therapy in that stable disease rather than disease regression might be the more typical response to successful intervention. Furthermore, it is possible that the cell cycle arrest produced by EGFR-directed therapy could affect the outcome of combination therapy with conventional cytotoxic agents (gemcitabine, taxanes, etc.) that tend to act on cells at later stages in the cell cycle (45–47). Importantly, we have obtained evidence that G_1-arrested cells may be more sensitive to apoptosis induced by tumor necrosis factor–related apoptosis-inducing ligand (TRAIL; ref. 48), a cytotoxic cytokine that is currently being evaluated in phase I clinical trials. Indeed, we have confirmed that gefitinib induces synergistic cell killing when it is combined with TRAIL in EGFR-dependent cell lines *in vitro* (49).[4]

Table 4. Quantification of immunohistochemical staining

	Absorbance* (mean ± SD)				
	p-EGFR	EGFR	TGF-α	p-Akt	p-MAPK
L3.6p1					
Control	1.7 ± 0.5	1.5 ± 0.2	2.3 ± 0.9	1.7 ± 0.3	3 ± 0.6
ZD1839	0.5 ± 0.2†	1.5 ± 0.7	1.2 ± 0.4†	0.7 ± 0.1†	0.3 ± 3.4†
MiaPaCa-2					
Control	1.2 ± 0.5	0.8 ± 0.2	0.6 ± 0.1	1.5 ± 0.5	1.5 ± 0.5
ZD1839	1.3 ± 0.5	0.7 ± 0.5	0.7 ± 0.1	1.8 ± 0.5	1.5 ± 0.4

*The absorbance of six positive cells per field in 10 random 0.159 mm^2 fields at ×100 magnification of different tumor tissues were measured using Image Quant analyzer and Optima Image software.
†$P < 0.001$ compared with the control group.

Perhaps not surprisingly, we observed significant levels of ERK and AKT phosphorylation in our cell lines regardless of whether or not they were gefitinib sensitive. However, in the sensitive cells, ERK and AKT phosphorylation were not further increased by exogenous EGF but were exquisitely sensitive to gefitinib, whereas EGF produced strong increases in ERK and AKT phosphorylation in the resistant cells, yet baseline phosphorylation of the kinases was completely insensitive to gefitinib. These observations are perfectly consistent with our hypothesis that EGFR-mediated signaling networks are "on" in the gefitinib-sensitive cells and "off" in the resistant ones, driven by availability of autocrine ligand production. Interestingly, ERK and AKT phosphorylation do not seem to correlate with the presence of activating K-ras mutations, in that BxPC3 is the only cell line in our panel that retains wild-type K-ras. We would expect that direct targeting of the ERKs and/or AKT would produce more global effects on tumor growth than are observed by targeting EGFR alone, but these strategies also seem to be associated with more systemic toxicity (49, 50). It is tempting to speculate that other autocrine growth factor–growth factor receptor interactions are required for cell cycle progression in some or most of the gefitinib-insensitive cell lines within our panel. Identifying them could yield additional therapeutic targets.

In conclusion, we have shown that the antiproliferative activity of gefitinib in human pancreatic cancer cell lines is linked to TGF-α production and inhibition of EGFR-mediated signaling but does not correlate with the degree of EGFR expression. Prospectively identifying potentially responsive tumors by their expression of TGF-α and exploiting the cytostatic effects of this class of drugs by combining them with TRAIL and other agents that preferentially kill G_1-arrested tumor cells may represent promising new approach to the treatment of pancreatic cancer.

Acknowledgments

Received 10/17/2005; revised 1/20/2006; accepted 1/30/2006.

Grant support: Regina Elena Cancer Institute and the M.D. Anderson Specialized Programs of Research Excellence (SPORE) in Pancreatic Cancer.

The costs of publication of this article were defrayed in part by the payment of page charges. This article must therefore be hereby marked *advertisement* in accordance with 18 U.S.C. Section 1734 solely to indicate this fact.

We thank Isaiah J. Fidler for critical review of the manuscript; Menashe Bar-Eli for providing the specific primers for exons 18 to 21 used in this study; Yasemin D. Yazici for her helpful advice; and Carol Oborn, Donna Reynolds, and Joseph Douglas for their assistance with histology and immunohistochemistry used in this study.

References

1. Jorissen RN, Walker F, Pouliot N, Garrett TP, Ward CW, Burgess AW. Epidermal growth factor receptor: mechanisms of activation and signalling. Exp Cell Res 2003;284:31–53.
2. Yarden Y, Sliwkowski MX. Untangling the ErbB signalling network. Nat Rev Mol Cell Biol 2001;2:127–37.
3. Earp HS, Dawson TL, Li X, Yu H. Heterodimerization and functional interaction between EGF receptor family members: a new signaling paradigm with implications for breast cancer research. Breast Cancer Res Treat 1995;35:115–32.
4. Wells A. EGF receptor. Int J Biol Cell Biol 1999;31:637–43.
5. Olayioye MA, Neve RM, Lane HA, Hynes NE. The ErbB signaling network: receptor heterodimerization in development and cancer. EMBO J 2000;19:3159–67.
6. Ennis BW, Lippman ME, Dickson RB. The EGF receptor system as a target for antitumor therapy. Cancer Invest 1991;9:553–62.
7. Kondapaka SB, Fridman R, Reddy KB. Epidermal growth factor and amphiregulin up-regulate matrix metalloproteinase-9 (MMP-9) in human breast cancer cells. Int J Cancer 1997;70:722–6.
8. Salomon DS, Brandt R, Ciardiello F, Normanno N. Epidermal growth factor-related peptides and their receptors in human malignancies. Crit Rev Oncol Hematol 1995;19:183–232.
9. Rubin Grandis J, Melhem MF, Gooding WE, et al. Levels of TGF-α and EGFR protein in head and neck squamous cell carcinoma and patient survival. J Natl Cancer Inst 1998;90:824–32.
10. Yamanaka Y, Friess H, Kobrin MS, Buchler M, Beger HG, Korc M. Coexpression of epidermal growth factor receptor and ligands in human pancreatic cancer is associated with enhanced tumor aggressiveness. Anticancer Res 1993;13:565–9.
11. Barton CM, Hall PA, Hughes CM, Gullick WJ, Lemoine NR. Transforming growth factor α and epidermal growth factor in human pancreatic cancer. J Pathol 1991;163:111–6.
12. Korc M, Chandrasekar B, Yamanaka Y, Friess H, Buchier M, Beger HG. Overexpression of the epidermal growth factor receptor in human pancreatic cancer is associated with concomitant increases in the levels of epidermal growth factor and transforming growth factor α. J Clin Invest 1992;90:1352–60.
13. Wagner M, Cao T, Lopez ME, et al. Expression of a truncated EGF receptor is associated with inhibition of pancreatic cancer cell growth and enhanced sensitivity to cisplatinum. Int J Cancer 1996;68:782–7.
14. Friess H, Wang L, Zhu Z, et al. Growth factor receptors are differentially expressed in cancers of the papilla of vater and pancreas. Ann Surg 1999;230:767–74.
15. Brehmer D, Greff Z, Godi K, et al. Cellular targets of gefitinib. Cancer Res 2005;65:379–92.
16. Giaccone G, Herbst RS, Manegold C, et al: Gefitinib in combination with gemcitabine and cisplatin in advanced non-small-cell lung cancer: a phase III trial-INTACT1. J Clin Oncol 2004;22:777–84.
17. Herbst RS, Giaccone G, Schiller JH, et al. Gefitinib in combination with paclitaxel and carboplatin in advanced non-small-cell lung cancer: a phase III trial-INTACT2. J Clin Oncol 2004;22:785–94.
18. Twombly R. Failing survival advantage in crucial trial, future of Iressa in jeopardy. J Natl Cancer Inst 2005;97:249–50.
19. Lynch TJ, Bogart JA, Curran WJ, Jr., et al. Activating mutations in the epidermal growth factor receptor underlying responsiveness of non-small-cell lung cancer to gefitinib. N Engl J Med 2004;350:2129–39.
20. Paez JG, Janne PA, Lee JC, et al. EGFR mutations in lung cancer: correlation with clinical response to gefitinib therapy. Science 2004;304:1497–500.
21. Barber TD, Vogelstein B, Kinzler KW, Velculescu VE. Somatic mutations of EGFR in colorectal cancers and glioblastomas. N Engl J Med 2004;351:2883.
22. Redlinger M, Kramer A, Flaherty K, Sun W, Halter D, O'Dwyer P. A phase II trial of gefitinib in combination with 5-FU/LV/irinotecan in patients with colorectal cancer. J Clin Oncol 2004;22:3767.
23. Bruns CJ, Harbison MT, Kuniyasu H, Eue I, Fidler IJ. *In vivo* selection and characterization of metastatic variants from human pancreatic adenocarcinoma by using orthotopic implantation in nude mice. Neoplasia 1999;1:50–62.
24. Nicoletti I, Migliorati G, Pagliacci MC, Grignani F, Riccardi C. A rapid and simple method for measuring thymocyte apoptosis by propidium iodide staining and flow cytometry. J Immunol Methods 1991;139:271–9.
25. Shi SR, Key ME, Kalra KL. Antigen retrieval in formalin-fixed, paraffin-embedded tissues: an enhancement method for immunohistochemical staining based on microwave oven heating of tissue sections. J Histochem Cytochem 1991;6:741–8.
26. Wu X, Rubin M, Fan Z, et al. Involvement of p27Kip1 in G_1 arrest mediated by an anti-epidermal growth factor receptor monoclonal antibody. Oncogene 1997;12:1397–403.
27. Peng D, Fan Z, Lu Y, DeBlasio T. Anti-epidermal growth factor receptor monoclonal antibody 225 up-regulates p27KIP1 and induces G_1 arrest in prostatic cancer cell line DU145. Cancer Res 1996;56:3666–9.
28. Huang SM, Bock JM, Harari PM. Epidermal growth factor receptor blockade with C225 modulates proliferation, apoptosis, and radiosensitivity in squamous cell carcinomas of the head and neck. Cancer Res 1999;59:1935–40.
29. Chan KC, Knox WF, Gee JM, et al. Effect of epidermal growth factor receptor tyrosine kinase inhibition on epithelial proliferation in normal and premalignant breast. Cancer Res 2002;62:122–8.
30. Ng SSW, Tsao M-S, Nicklee T, Hedley DW. Effects of the epidermal growth factor receptor inhibitor OSI-774, Tarceva, on downstream signaling pathways and apoptosis in human pancreatic adenocarcinoma. Mol Cancer Ther 2002;1:777–83.
31. Janmaat ML, Kruyt FA, Rodriguez JA, Giaccone G, Janmaat ML. Response to epidermal growth factor receptor inhibitors in non-small cell lung cancer cells: limited antiproliferative effects and absence of apoptosis associated with persistent activity of extracellular signal-regulated kinase or Akt kinase pathways. Clin Cancer Res 2003;9:2316–26.
32. Campiglio M, Locatelli A, Olgiati C, et al. Inhibition of proliferation and induction of apoptosis in breast cancer cells by the epidermal growth factor receptor (EGFR) tyrosine kinase inhibitor ZD1839 ("Iressa") is independent of EGFR expression level. Cell Physiol 2004;198:259–64.
33. Mendelson J. Targeting the epidermal growth factor receptor for cancer therapy. J Clin Oncol 2002;15:1s–13.
34. Saltz LB, Meropol NJ, Loehrer PJ, Sr., Needle MN, Kopit J, Mayer RJ. Phase II trial of cetuximab in patients with refractory colorectal cancer that expresses the epidermal growth factor receptor. J Clin Oncol 2004;22:1201–8.
35. Moasser MM, Basso A, Averbuch SD, Rosen N. The tyrosine kinase inhibitor ZD1839 ("Iressa") inhibits HER-2-driven signaling and suppresses the growth of HER2 overexpressing tumor cells. Cancer Res 2001;61:7184–8.
36. Moulder SL, Yakes FM, Muthuswamy SK, Bianco R, Simpson JF, Arteaga CL. Epidermal growth factor receptor (HER1) tyrosine kinase inhibitor ZD1839 (Iressa) inhibits HER2/neu (erbB2)-overexpressing breast cancer cells *in vitro* and *in vivo*. Cancer Res 2001;61:8887–95.
37. Magne N, Fischel JL, Dubreuil A, et al. Influence of epidermal growth factor receptor (EGFR), p53, and intrinsic MAP kinase pathway status of tumour cells on

the antiproliferative effect of ZD1839 ("Iressa"). Br J Cancer 2002;86:1518–23.
38. Bruns CJ, Harbison MT, David DW, et al. Epidermal growth factor receptor blockade with C225 plus gemcitabine results in regression of human pancreatic carcinoma growing orthotopically in nude mice by antiangiogenic mechanisms. Clin Cancer Res 2000;6: 1936–48.
39. Baker CH, Kedar D, McCarty MF, et al. Blockade of epidermal growth factor receptor signaling on tumor cells and tumor-associated endothelial cells for therapy of human carcinomas. Am J Pathol 2002;161:929–38.
40. Jemal A, Murray T, Ward E, et al. Cancer statistics, 2005. CA Cancer J Clin 2005;55:10–30.
41. Burris HA III, Moore MJ, Andersen J, et al. Improvements in survival and clinical benefit with gemcitabine as first-line therapy for patients with advanced pancreas cancer: a randomized trial. J Clin Oncol 1997;15:2403–13.
42. Xiong HQ, Rosenberg A, LoBuglio A, et al. Cetuximab, a monoclonal antibody targeting the epidermal growth factor receptor, in combination with gemcitabine for advanced pancreatic cancer: a multicenter Phase II Trial. J Clin Oncol 2004;22:2610–6.
43. Arteaga CL. Trastuzumab, an appropriate first-line single-agent therapy for HER2-overexpressing metastatic breast cancer. Breast Cancer Res 2003;5:96–100.
44. Vogel CL, Cobleigh MA, Tripathy D, et al. Efficacy and safety of trastuzumab as a single agent in first-line treatment of HER2-overexpressing metastatic breast cancer. J Clin Oncol 2002;20:719–26.
45. Plunkett W, Huang P, Xu YZ, Heinemann V, Grunewald R, Gandhi V. Gemcitabine: metabolism, mechanisms of action, and self-potentiation. Semin Oncol 1995;22:3–10.
46. Verweij J, Clavel M, Chevallier B. Paclitaxel (Taxol) and docetaxel (Taxotere): not simply two of a kind. Ann Oncol 1994;5:495–505.
47. Schiff PB, Fant J, Horwitz SB. Promotion of microtubule assembly *in vitro* by Taxol. Nature 1979; 277:665–7.
48. Lasingher LM, Zhu K, Williams SA, Shrader M, Dinney CP, McConkey DJ. Bortezomib abolishes tumor necrosis factor-related apoptosis-inducing ligand resistance via a p21-dependent mechanism in human bladder and prostate cancer cells. Cancer Res 2005;65: 4902–8.
49. Fuminori T, Shunsuke K, Takanori W, et al. ZD1839 (Gefitinib, Iressa), an epidermal growth factor receptor-tyrosine kinase inhibitor, enhances the anti-cancer effects of TRAIL in human esophageal squamous cell carcinoma. FEBS Lett 2005;579:4069–75.
50. Cohen SJ, Ho L, Ranganathan S, et al. Phase II and pharmacodynamic study of the farnesyltransferase inhibitor R115777 as initial therapy in patients with metastatic pancreatic adenocarcinoma. J Clin Oncol 2003;21:1301–6.

Published OnlineFirst December 1, 2009; DOI: 10.1158/0008-5472.CAN-09-4221

Correction

Cancer Research

Correction: Transforming Growth Factor α Expression Drives Constitutive Epidermal Growth Factor Receptor Pathway Activation and Sensitivity to Gefitinib (Iressa) in Human Pancreatic Cancer Cell Lines

In this article (Cancer Res 2006;66(7):3802-12) published in the April 1, 2006 issue of *Cancer Research* (1), an error was made in Fig. 5*B*. The same image was used to represent pMAPK expression in control samples from both MiaPaCa-2 and L3.6pl tumor xenografts and the image intensity/contrast was significantly altered. The panels in question are shown below:

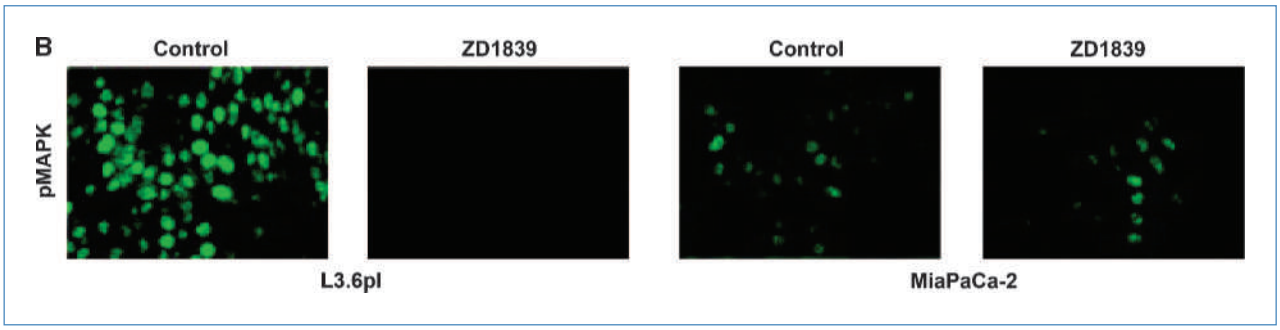

The authors have corrected the figure and regret their error. The corrected Fig. 5*B* appears below:

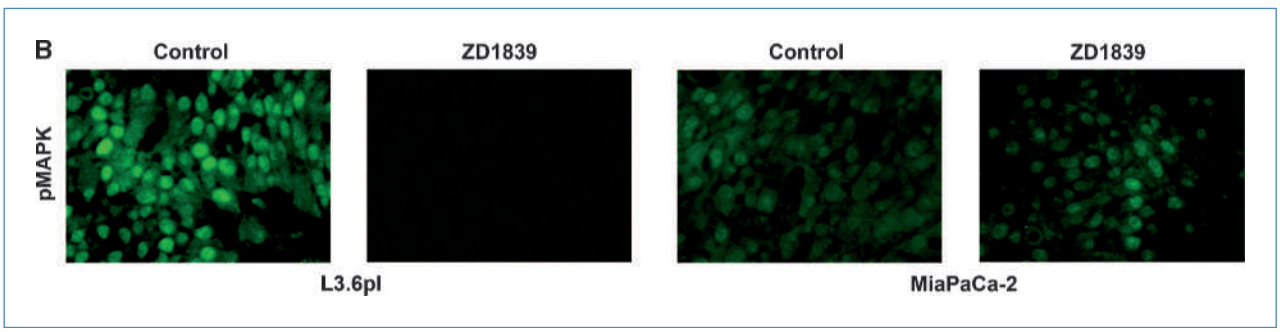

Corrections for several articles published in AACR journals containing similar errors have been published. The original articles and their corrections are:

Nawrocki ST, Carew JS, Pino MS, Highshaw RA, Dunner K, Jr., Huang P, Abbruzzese JL, McConkey DJ. Bortezomib sensitizes pancreatic cancer cells to endoplasmic reticulum stress-mediated apoptosis. Cancer Res 2005;65:11658-66. doi:10.1158/0008-5472.CAN-05-2370.

Correction In: Cancer Res 2009;69:1695. Published OnlineFirst February 10, 2009. doi: 10.1158/0008-5472.CAN-69-4-COR1.

Nawrocki ST, Bruns CJ, Harbison MT, Bold RJ, Gotsch BS, Abbruzzese JL, Elliott P, Adams J, McConkey DJ. Effects of the proteasome inhibitor PS-341 on apoptosis and angiogenesis in orthotopic human pancreatic tumor xenografts. Mol Cancer Ther 2002;1:1243-53.

Correction In: Mol Cancer Ther 2009;8:3388-9. Published OnlineFirst December 1, 2009. doi: 10.1158/1535-7163.MCT-09-1072.

Nawrocki ST, Sweeney-Gotsch B, Takamori R, McConkey DJ. The proteasome inhibitor bortezomib enhances the activity of docetaxel in orthotopic human pancreatic tumor xenografts. Mol Cancer Ther 2004;3:59-70.

Correction In: Mol Cancer Ther 2009;8:479. Published OnlineFirst February 3, 2009. doi: 10.1158/1535-7163.MCT-08-2-COR1.

Papageorgiou A, Kamat A, Benedict WF, Dinney C, McConkey DJ. Combination therapy with IFN-alpha plus bortezomib induces apoptosis and inhibits angiogenesis in human bladder cancer cells. Mol Cancer Ther 2006;5:3032-41. doi: 10.1158/1535-7163.MCT-05-0474.

Correction In: Mol Cancer Ther 2009;8:480. Published OnlineFirst February 3, 2009. doi: 10.1158/1535-7163.MCT-08-2-COR2.

The errors in the aforementioned articles were caused in large part by inadequate oversight of data management. In an effort to prevent such errors from occurring in the future, the PI (DJM) has implemented a new data management policy that is designed to limit or eliminate errors in future publications, and would be happy to provide it to anyone interested upon request (dmcconke@mdanderson.org). The authors note that the conclusions and interpretation of the data in these articles are unaltered by the errors that are now corrected.

Reference

1. Pino MS, Shrader M, Baker CH, Cognetti F, Xiong HQ, Abbruzzese JL, McConkey DJ. Transforming growth factor α expression drives constitutive epidermal growth factor receptor pathway activation and sensitivity to gefitinib (Iressa) in human pancreatic cancer cell lines. Cancer Res 2006;66:3802–12. doi: 10.1158/0008-5472.CAN-05-3753.

Published OnlineFirst 12/1/09.

doi: 10.1158/0008-5472.CAN-09-4221

Transforming Growth Factor α Expression Drives Constitutive Epidermal Growth Factor Receptor Pathway Activation and Sensitivity to Gefitinib (Iressa) in Human Pancreatic Cancer Cell Lines

Maria S. Pino, Marissa Shrader, Cheryl H. Baker, et al.

Cancer Res 2006;66:3802-3812.